3

The Prediction of Acid Mine Drainage Potential Using Mineralogy

Deshenthree Chetty*, Olga Bazhko, Veruska Govender and Samuel Ramatsoma

Mintek, Randburg, South Africa

Abstract

The generation of acid mine drainage (AMD) occurs through oxidation of sulfide minerals exposed to air and water, a process exacerbated by mining and extraction activities. Although the assessment of AMD potential is often performed through static geochemical tests, mineralogical information produces complementary data to more thoroughly assess the risk of AMD formation. This chapter focuses on mineralogy and geochemistry as tools to generate input for the formulation of AMD prediction models, specifically addressing mineral acid formation and consumption potential, mineral abundance, mineral reactivity, and mineral liberation in process wastes. Mineral liberation is defined here as the amount of mineral surface exposed to make the mineral amenable to reaction with air, water, or acidic solutions. Adding a mineral liberation parameter builds on previous models for the prediction of AMD potential of wastes. These newly developed models were applied to gold and copper ore process residues and results compared with traditional static geochemical test results. Both, the effects of modal mineralogy and mineral liberation were further evaluated for two base metal sulfide (BMS) tailings compositions. To conclude, this predictive approach lends itself to improved process design and better-informed waste management strategies to mitigate detrimental effects of AMD, as part of a geometallurgical program, with possibilities to extend into prediction of AMD potential over time. In this respect, when applied to waste rocks, the predictive approach could be a desirable alternative to time-consuming and costly kinetic tests.

Keywords: Acid mine drainage, prediction, mineralogy

3.1 Introduction

Sustainable use of natural resources is a long-held ideal for the mining and ore processing industries. When adequate sustainability measures are not implemented, environmental and social issues arise that require urgent attention [1]. Acid mine drainage (AMD) is one such issue, for which several treatment options have been developed, but which remains a formidable challenge worldwide. A geometallurgical approach to the mining and processing of ores reduces technical, economic, environmental, and social risk for operations and

**Corresponding author*: deshc@mintek.co.za [ORCID: 000-0002-1913-7598]
[ORCID: Bazhko, 000-0002-1598-0123; Govender, 000-0001-6848-6527; Ramatsoma, 000-0002-8079-8424]

Elvis Fosso-Kankeu, Christian Wolkersdorfer and Jo Burgess (eds.) Recovery of Byproducts from Acid Mine Drainage Treatment, (49–72)

therefore must incorporate sustainability as a key aspect. The approach relies on a high confidence in predictive capability, which is underpinned by an understanding of the orebody with respect to how it will be mined and processed to reduce such risks. As part of a predictive approach, not only the process efficiencies must be considered, but also the management of waste that will be generated from mining and processing of the ore, to reduce environmental and, by extension, social and economic risk.

Mineralogy is a key factor in considering value extraction from an orebody. In this respect, the relationship between ore and gangue minerals is important for determining appropriate process flowsheet options. Such options must provide optimized grades and recoveries to concentrates that will be further refined through e.g., smelting or hydrometallurgical process routes. While concentrates must meet certain specifications, the same is not necessarily true for the wastes generated at each step in the concentration process.

Acid mine drainage is the detrimental consequence of inadequate planning for the release of acid (defined as H_2SO_4 in this study) and metals from the oxidation of (di-)sulfide minerals present in the ore, a natural process that is exacerbated by mining and processing [2–5]. This results from each step of the mining and processing chain of activities, in which rock is broken up into progressively smaller particles, leading to increased exposure of (di-) sulfide minerals to air and water. Consequently, this leads to increased mineral surface area that is amenable to oxidation. Whereas value-bearing sulfides are largely extracted through processing, non-value-bearing sulfides remain in waste products and will be subject to oxidation, which is accelerated by bacteria [4]. The mitigation of such effects is aided by the presence of associated, potentially neutralizing minerals in the ore [4]. It is therefore evident that mineralogy must play an integral role in sustainable use of the resource.

Presently, much of the effort in addressing AMD generation in South Africa is targeted at remedial processes to reverse the damage already done [6–8], but lesser attention has been given to prediction and prevention of AMD generation and associated metal contamination in the environment. Yet, predictive capabilities would be of benefit not only to new operations, but also brownfield expansion programs, and indeed, waste already generated from ongoing and spent operations.

Over the last two decades, many strides have been made in complementing traditional geochemical techniques like static acid-base-accounting (ABA) methods, as well as kinetic geochemical tests, with mineralogical characterization of waste rock materials [5, 9–15]. The mineralogical characterization has included modal mineralogy and increasingly quantitative assessment of mineral association in defining lithotypes [9, 16], assessing accuracy of static geochemical tests [11], and understanding reactions in kinetic tests [10, 17, 18] in predicting AMD potential.

In many of these instances, liberation of minerals, whether sulfides or other minerals, has not been given much attention. Mineral liberation describes the degree of surface exposure of the mineral, i.e., the amount of mineral grain surface that is amenable to interaction with air, water, or other reactants. Only a few instances have recently been shown where mineral liberation is reported from automated scanning electron microscopy (SEM) [17, 18] in the context of AMD studies. However, these data have not been expressly incorporated into a descriptor for AMD potential or risk. Mineral liberation is a function of the particle size of rock, and in macro-scale observations [9] of a few centimeters to meter-sized rocks, sulfide mineral liberation will not play an overtly large role for acid production, as the particle size is much larger than the constituent mineral grain size, resulting in partial exposure of

the mineral grains for reaction. However, where particles occur at the micrometer-scale of observation (i.e., the typical particle size after processing to extract valuable sulfide), liberation of the same constituent mineral grains will increase, and therefore, mineral liberation becomes more important for the mineral reactivity. In the base metal sulfide (BMS) and gold mining industries, the waste generated from such processes as physical separation, flotation, and leaching generally contains notable concentrations of sulfide minerals that may oxidize and release metal contaminants.

This chapter therefore describes the use of modal mineralogy and mineral liberation data in the calculation of acid production and neutralization potential (NP), specifically with regard to process wastes, for the prediction of AMD risk. The chapter further briefly discusses the incorporation of such efforts in geometallurgical programs, including mineralogical prediction as a potential alternative to kinetic testing. In the latter case, the application of mineralogical studies to ores and waste rock can be coupled with mine planning and spatial distribution of potential acid forming rock types to inform not only mine production efficiency but also the potential for wastes to form AMD over time. Temporal aspects include when each rock type will be mined and, from there on, when AMD can be expected to be released, as well as the rate at which this release can take place.

3.2 Mineralogical Approach for Prediction of AMD Potential

In applying a mineralogical approach for prediction of AMD potential, various factors must be considered. The first is maximum potential of minerals to form or consume acid, the second is the proportion of such minerals in the sample, and the third is the mineral reactivity. An additional parameter, liberation, is considered in this contribution. These aspects are individually discussed in the sections below.

3.2.1 AMD Chemistry for Maximum Acid Generation or Consumption Potential

The AMD potential of waste is the balance between the acid potential (AP) of the waste, determined by the acid-producing components, and the NP, determined by the acid-consuming components. Generally, the evaluation of AMD potential involves static geochemical tests to ascertain the potentially acidic and alkaline nature of samples [19–22]. Classification of AMD potential is based on the ratio of AP and NP, derived from such tests. Commonly used static procedures for characterization of mining wastes to predict AMD are the ABA test procedure of Sobek *et al.* [19] and its modified version [20, 21]. In the method of Sobek *et al.* [19] the AP of a sample is determined by calculation of the theoretical amount of acid that can be produced if the total amount of sulfur in the sample is oxidized to form sulfuric acid. The NP of the sample is determined experimentally by digestion in excess hydrochloric acid at boiling, and back titration of remaining acid to pH 7. The disadvantage of the Sobek method is the overestimation of AP and NP values [22, 23]. The modified Sobek procedure of Lawrence [20] determines NP at lower temperature, with the end point of back titration being pH 8.3, which prevents overestimation of NP. This modified procedure uses sulfide, as opposed to total sulfur, for the AP calculation [23]. Lapakko [22] proposed measuring NP by the amount of acid reacted with a sample to

achieve a stable pH 6. This conservatively determined the required NP to meet water quality standards, which typically require pH in excess of 6, and showed better accuracy than the Sobek *et al.* [19] procedure.

The chemistry of AMD generation can be complex, as various environmental factors can influence chemical reactions, which will result in different products. For example, metal ions such as Fe^{3+}, released during (di-)sulfide oxidation, along with Al^{3+}, may hydrolyze, releasing additional acid. Therefore, pyrite oxidation may be described by the following equations [24]:

$$FeS_2 + 7/2\ O_2 + H_2O \rightarrow Fe^{2-} + 2\ SO_4 + 2\ H^+ \tag{3.1}$$

$$Fe^{2+} + 1/4\ O_2 + H_+ \rightarrow Fe_{3+} + 1/2\ H_2O \tag{3.2}$$

$$Fe^{3+} + 3\ H_2O \rightarrow Fe(OH)_3 + 3\ H^+ \tag{3.3}$$

Other sulfides show different acid-producing potential. Iron-bearing sulfides readily generate acidity, whereas sulfides that do not contain Fe in their crystal lattices (e.g., galena, PbS) are not capable of generating substantial acid [25–27]. Sulfides like sphalerite [(Zn,Fe)S], which can show solid solution substitution of Zn^{2+} with Fe^{2+}, will either not produce acid upon oxidation or can produce considerable acid with increased Fe^{2+} content [28].

The precipitation of Fe^{3+} and Al^{3+} hydroxides is a substantial source of acidity in mine waste [11]. Secondary Fe^{3+}-hydroxy-sulfate minerals (e.g., schwertmannite, $Fe_{16}O_{16}(OH)_{12}(SO_4)_2$; jarosite, $KFe_3(SO_4)_2(OH)_6$) commonly occur in pyrite or pyrrhotite ($Fe_{1-x}S$) mine waste [5], and dissolution or precipitation of these phases is potentially acid-producing (Eq. 3.4).

$$KFe_3(SO_4)_2\ (OH)_6 + 3\ H_2O \rightarrow 3\ Fe(OH)_3 + K^+ + 3\ H^+ + 2\ SO_4^{2-} \tag{3.4}$$

Acid produced by (di-)sulfide oxidation can be consumed during reaction with gangue minerals. Neutralization is primarily achieved through dissolution of carbonate minerals; calcite ($CaCO_3$) is the most effective at this [12]. Some neutralization can be achieved from silicate mineral dissolution, particularly the dissolution of olivine [$(Mg,Fe)_2SiO_4$], serpentine [$(Mg,Fe)_3Si_2O_5(OH)_4$], and wollastonite ($CaSiO_3$), as well as clay minerals, mica (Eq. 3.5) and calcic plagioclase (Eq. 3.6). However, practical NP values can be much lower than expected, as the contributions are minimized from those acid neutralizing minerals that would dissolve only under acidic conditions, i.e., such minerals are relatively stable under neutral conditions.

$$KAl_2[AlSi_3O_{10}](OH)_2 + H^+ + 3/2\ H_2O \rightarrow K^+ + 3/2\ Al_2Si_2O_5(OH)_4 \tag{3.5}$$

$$CaAl_2Si_2O_8 + 2\ H^+ + H_2O \rightarrow Ca^{2+} + Al_2Si_2O_5(OH)_4 \tag{3.6}$$

Identified minerals are broadly grouped as acid forming, acid consuming or buffering, and inert [4, 29–34]. Acid formers include most sulfides, which react with oxygen and water to produce metal cations, sulfate and H^+. The process is, however, a complex, multistage

one, as indicated above, and can include metal cation oxidation and hydrolysis, during which precipitates may be formed.

In building on mineralogical-based protocols for the prediction of AMD potential, acid formation (and acid consumption) of different minerals are considered, as per previous workers [11, 15, 27]. Acid formation (or consumption) is calculated according to Eq. 3.7:

$$\text{AP} = \text{acid formation (consumption)} \times 98.097 \times \text{molecular mass of mineral} \times 1{,}000 \tag{3.7}$$

Where

AP = acid production potential of the mineral, based on its oxidation (or acid consumption) reaction, in kg H_2SO_4/t;
acid formation (consumption) is in mol acid per mol mineral reacted;
98.097 is the molecular mass of H_2SO_4, in g mol^{-1};
molecular mass of the mineral is in g mol^{-1};
1,000 is the factor to convert to kg H_2SO_4/t.

This parameter is therefore solely a descriptor of the amount of acid that is formed per mol of mineral that reacts; alternatively, it is the amount of acid that is consumed per mol of mineral that reacts, as in the case of carbonates. Positive values indicate acid production, whereas negative values indicate acid consumption, based on the reactions involved. To simplify geochemical reactions and calculate acid formation potential, complete oxidation and formation of products and a neutral pH have been assumed in the present calculations. The chemical reactions and acid formation or consumption for assessed minerals show that Fe^{2+}, Sb^{3+}, and As^{3+} containing sulfides generate notable acid, compared with BMS minerals lacking these elements [35]. Examples are provided with arsenopyrite (Eq. 3.8) and galena (Eq. 3.9), which have acid production potentials of 601 kg/t H_2SO_4 and 0, respectively, as per Eq. 3.7.

$$2\,FeAsS + 7\,O_2 + 2\,H_2O \rightarrow 2\,FeAsO_4 + 2\,H_2SO_4 \tag{3.8}$$

$$PbS + 2\,O_2 \rightarrow PbSO_4 \tag{3.9}$$

Tailings from metallurgical processes often contain metal hydroxyl sulfates (particularly Fe^{3+} and Al^{3+}) that may also release acid. On the other hand, carbonate, phosphate, and some hydroxide and oxide minerals will consume acid. Silicate alteration reactions will all be acid consuming, as metals are replaced by H^+ with cation release in the forms of the metal cation (e.g., K^+, Ca^{2+}, Na^+), oxidation (of Fe^{2+}) and hydrolysis (Fe^{3+} and Al^{3+}), with potential formation of more stable minerals like clays [36].

For the evaluation of AMD potential, complete hydrolysis reactions with formation of SiO_2 and metal salts or hydroxides are assumed. It should be highlighted that the reactions make available the maximum NP of the mineral. However, the NP offered by these reactions is often not attained because mineral dissolution is commonly accompanied by neoformed phases [37]. The nature of the neoformed phases is dependent on the abundance, composition, and chemical properties of the solution. The latter include Eh, pH, and solute concentration.

3.2.2 Mineral Modal Abundance

In order to calculate the amount of acid that may be produced (or consumed) by the mineral as part of its contribution to the total behavior of the sample, consideration is given to the proportion of minerals present in the sample [15]. The mass proportions of key acid producers (i.e., sulfides) and consumers (i.e., carbonates) may then be determined by such mineralogical techniques as quantitative X-ray diffraction, using Rietveld refinement. Other gangue minerals like silicates are also quantified by this method. However, the technique, while rapid, suffers from high detection limits, and so automated SEM techniques like QEMSCAN (Quantitative Evaluation of Minerals using Scanning Electron Microscopy) [38], MLA (Mineral Liberation Analyzer) [39], and Mineralogic [17], among others, may be used [11, 13, 17, 18]. These methods provide typical detection limits of 0.1 mass% of mineral present.

3.2.3 Mineral Reactivity

Mineral reactivity is the third aspect to consider in determining propensity for the sample to produce (or consume) acid. Therefore, not only the total amount of each mineral consuming or producing acid, but also the rate at which acid generation or neutralization will occur, must be determined. Different minerals have different reactivities. Carbonate minerals such as calcite ($CaCO_3$) and dolomite [$CaMg(CO_3)_2$] are the most effective neutralizing minerals because they have relatively high reactivities and neutralize acidity over a wide pH range. For low reactivity minerals, their presence in a waste will not necessarily provide protection against AMD if the rate of neutralization is lower than the rate of acid generation. Silicate minerals can be important neutralizers because of their abundance, but their relative reactivity ranges from intermediate to extremely slow relative to that of carbonates.

Sverdrup [40] suggested that minerals can be divided into different groups (carbonate, silicates, and others) in order of relative reactivity in acidic solution (Table 3.1), with the reaction rates at pH 5.0 relative to a calcite reactivity of 1.00 as calculated by Kwong [41]. Sulfides are not listed in this scheme.

The abrasion pH value has been previously used for comparing the reactivity of acid generating and neutralizing minerals. Noble and Lottermoser [42] measured the abrasion pH value for a wide variety of minerals. To convert the abrasion pH to reactivity, Parbhakar-Fox *et al.* [11] used the deviation of the pH value from a $CaCl_2$ solution with pH 6.4. According to this normalization of the abrasion pH values, BMS minerals should have low reactivity, which is not reflected by reality. These minerals are oxidized but may not necessarily produce acid. The oxidation, however, results in sulfate and metal release, which contributes to toxicity and is important to consider for AMD generation.

Alternative approaches were adopted by Bouzahzah *et al.* [43] and Chopard *et al.* [27, 44] for determining sulfide oxidation rates as a measure of sulfide reactivity. The approach proposed by Chopard *et al.* [44] is preferred for determining sulfide reactivity, as it is based on measurements of oxidation rates of various sulfide minerals, which consider mass and surface area of individual sulfides of different compositions. Table 3.2 shows the results for sulfide mineral oxidation from their work, along with relative reactivity calculated from their data. The relative reactivity can be calculated by assigning a reactivity of 1 for pure pyrite.

Table 3.1 Reactivity of selected minerals [40, 41].

Mineral group	Typical minerals	Relative reactivity (at pH 5)
Dissolving	Calcite, aragonite, dolomite, magnesite, brucite	1.00
Fast weathering	Anorthite, nepheline, forsterite, olivine, garnet, jadeite, leucite, spodumene, diopside, wollastonite	0.6
Intermediate weathering	Sorosilicates (epidote, zoisite), pyroxenes (enstatite, hypersthene, augite, hedenbergite), amphiboles (hornblende, glaucophane, tremolite, actinolite, anthophyllite), phyllosilicates (serpentine, chrysotile, talc, chlorite, biotite)	0.4
Slow weathering	Plagioclase feldspars (albite, oligoclase, labradorite), clays (vermiculite, montmorillonite)	0.02
Very slow weathering	K-feldspars, muscovite	0.01
Inert	Quartz, rutile, zircon	0.004

It can be further noted that the same mineral may show different oxidation rates as a result of differing minor and trace element contents, e.g., pyrrhotite and pyrite [27]. Other sulfides, e.g., sphalerite, are prone to solid solution substitution of Zn^{2+} by Fe^{2+} and Mn^{2+}, which increase the oxidation rate. In this respect, it is worth investigating sulfide mineral compositions to assign appropriate reactivity, particularly where large concentrations of such minerals are evident. Thus, mineral chemistry, which is useful for understanding recovery and grade from processing of ores, could also prove useful for understanding oxidation of minerals in a tailings storage facility. Different compositions will be governed in part by the type of ore deposit in which the given sulfide occurs. The small database of Chopard *et al.* [44] is a useful start in this regard. In the current study, the reactivities of sulfides were calculated as per equation 1.10, based on the experimental results of these authors.

Table 3.2 Oxidation rate for selected (di-)sulfides and normalization to pyrite [44].

Mineral	$g/m^{-2}/day$	Normalized to pyrite = 1
pyrrhotite	0.638×10^{-3}	8.43
Fe sphalerite	1.51×10^{-4}	1.99
pyrite	7.57×10^{-5}	1.00
galena	6.52×10^{-5}	0.86
chalcopyrite	3.3×10^{-5}	0.44

$$\text{Reactivity of sulfide} = \text{sulfide oxidation rate/pyrite oxidation rate} \quad (3.10)$$

The relative reactivity for (di-)sulfides and non-sulfides applied in the calculation of AMD risk was therefore based on the data provided by Chopard *et al.* [44] and Kwong [41]. Where no data are available in the literature, assumptions were required, which will influence the accuracy of the data. It is noted that the reactivity of sulfides and carbonates or silicates are based on different mechanisms for reaction. In the case of sulfides, reactivity is based on the oxidation potential, whereas for carbonates and silicates, reactivity is the ability to react with acid. Where pyrite produces acid, calcite will immediately consume it, whereas silicates will take longer to do so. Thus, the scaling of relative reactivity is done with calcite and pyrite both at 1.

3.2.4 Mineral Liberation

A fourth aspect to be considered in AMD studies is mineral liberation, which has been used to interpret kinetic test results of waste rocks [17, 18]. Mineral liberation is expressed in two ways. The first is the mass of the mineral of interest (e.g., sulfide) as a proportion of the total mass of the particle in which it occurs. This is referred to as liberation by grade. Intuitively, liberation by grade will increase as the particle size decreases. Thus, liberation by grade may be defined as the degree to which particle size (also mass) and mineral grain size (also mass) assume unity. A completely liberated particle will be the same composition as the mineral grain, whereas a small mineral grain locked in a particle containing other, larger mineral grains, will assume a low grade approaching 0 (Figure 3.1).

The second way is liberation expressed as free surface or exposure, i.e., the proportion of the surface of the mineral that is exposed to the atmosphere. As per the example above, the small mineral grain locked in the particle will not have any exposed surface and will therefore not be amenable to oxidation (except through possible galvanic interactions where two sulfides are in direct contact) or acid-base reactions interaction, whereas the completely liberated mineral will have its entire surface available for reaction (Figure 3.1).

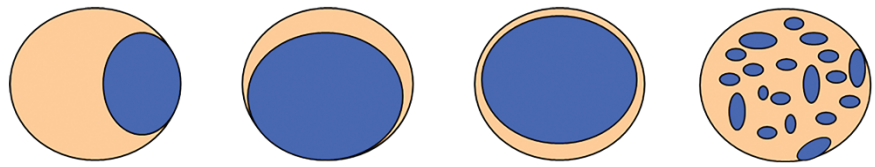

Figure 3.1 Liberation by grade and exposure concepts, using identical particle sizes (particles composed of dark and light minerals), but different mineral-of-interest grain size (dark) and location in the particle. The free or exposed surface of the dark mineral is the same in the first two images (≈45% of the dark total surface, expressed as perimeter in 2D), even though their liberation by grade is different (higher in the second image than in the first). The second and third images show identical liberation by grade (the areas of the dark mineral are the same) but very different liberation by exposure (≈45% versus 0). The last image shows an identical liberation by grade to the first image (same area covered by one grain versus several smaller grains of the dark mineral) but rather different liberation by exposure (<5% for the several smaller grains versus 45% for the single large grain).

Note that the two concepts are rather different but related. Both are very much dependent on the original texture of the ore versus the particle size to which it has broken. For example, an ore particle containing a finely disseminated sulfide mineral in a gangue matrix might have a higher liberation by grade value than a liberation by exposure value. This is because the mass of total sulfide may be more concentrated in the interior of the particle than at the surface, leading to lower exposure at the particle surface. Similarly, in the case of process wastes, passivation effects that prevent complete oxidation of minerals will likely result in high liberation by grade values but will give zero liberation by exposure (Figure 3.1). Generally, however, higher liberation by grade may be expected to yield higher liberation by exposure as particles are broken down.

Liberation by grade and by exposure are well-established descriptors derived from automated SEM. In this contribution, liberation by exposure is used, and this descriptor can be generated from a mineral association list, in which association with free surface (e.g., MLA) [39] or background (i.e., mounting medium of resin, QEMSCAN) [45] can be used.

3.2.5 Calculation of the AMD Potential

Oxidation of minerals for acid formation or acid consumption, as may be the case, relies on available mineral surface for reaction. It is therefore proposed here that liberation by exposure be included with the acid formation or consumption potential and mineral reactivity, to assess AMD risks. Using the information gleaned, an AMD value and an AMD ratio are calculated to assess the AMD potential (Eqs. 3.11 and 3.12):

$$\text{AMD value} = \text{AP} \times m \times \text{R} \times \text{L} \tag{3.11}$$

Where

the AMD value is the amount of H_2SO_4 produced, in kg/t;
m is the mass fraction of the mineral, i.e., mass%/100;
AP is the acid potential, calculated based on maximum acid generation/consumption (mol acid produced or consumed per mol mineral reacting), expressed as H_2SO_4 in kg/t;
R is the relative reactivity of the mineral;
L is the liberation of the mineral, i.e., %free surface/100.

$$\text{AMD ratio} = -\Sigma\text{AMD value (ACM)}/\Sigma\text{AMD value (AGM)} \tag{3.12}$$

Where

ACM are the acid consuming minerals;
AGM are the acid generating minerals.

The AMD value will be negative if the mineral consumes acid but will be positive if the mineral generates acid. If no acid is generated or consumed, the AMD value is 0. Similarly, if a mineral is not liberated, the AMD value is 0. The sum of all mineral AMD values will give the AMD value for the sample. Again, a positive AMD value would be obtained for a sample with acid generating potential whereas a negative value indicates acid-neutralizing

potential of the sample. A higher value (positive or negative) indicates a larger acid generation or neutralization capacity.

The AMD ratio assists in determining the risk of acid formation. It is ranked based on the correlation between the AMD ratios calculated for real samples with outcomes from environmental test work. Where the AMD ratio is <1, AMD risk is evident, where >1, no AMD risk is evident. This ratio differs from the CARD risk ratio of Parbhakar-Fox *et al.* [11] as it incorporates mineral liberation in the AMD value, in addition to mineral acid producing or consuming potential and mineral reactivity. In this way, a texture-based ABA protocol is better realized.

The steps for producing a liberation-based AMD ratio were therefore carried out for different process wastes as follows:

- identification and quantification of the modal proportions of acid-generating and neutralizing minerals in a sample using mineralogical techniques (QEMSCAN analysis);
- identification of maximum acid generation or consumption potential of these minerals based on chemical reactions involving the release or consumption of H_2SO_4;
- evaluation of mineral reactivity based on information available in published literature or obtained during gold leaching test work carried out at Mintek;
- assessment of mineral liberation to further evaluate availability for acid generation or neutralization;
- calculation of sample AMD values and ratios.

Comparison with ABA and Net Acid Generating (NAG) static geochemical results was additionally conducted on four residues.

An AMD predictor software package was further developed to take as inputs, the ABA and NAG geochemical data and the mineralogical data (mineral proportions, reactivity, and liberation). Generated outputs were the geochemical and mineralogical results, providing a quick comparison of traditional static geochemical tests and mineralogical-based AMD prediction.

3.3 Application of the AMD Predictive Protocol

High concern for AMD generation in South Africa emanates from its gold processing tailings, for which AMD treatment options are continuously tested. In this regard, QEMSCAN mineral modal abundance and liberation data, carried out on three residues from different gold processing projects (Au res 1, Au res 2, Au res 3), were assessed using the AMD predictive protocol. The results were compared with static geochemical tests conducted on those samples. Additionally, a copper-bearing residue (Cu res 1) was assessed for comparison against static geochemical tests. Two further compositions represent typical BMS process tailings that may be generated, a Zn tailing (BMS Tails 1) and a Ni tailing (BMS Tails 2). Together, the data are presented to illustrate the influence of liberation, modal mineral abundance, and mineral reactivity on the AMD value and ratio of different waste types.

3.3.1 Experimental Procedures

To facilitate modal analysis, the samples were screened into appropriate size fractions, with polished sections made from each fraction and subjected to particle mineral analysis (PMA) [38] using a QEMSCAN automated scanning electron microscope. At the particle size analyzed, more than 10,000 particles are typically scanned in each fraction from which polished sections are made. With at least four fractions derived, at least 40,000 particles are assessed over the full sample, ensuring good representivity. Mineral modal abundance and liberation data were extracted for the minerals identified, as a function of the total sample (i.e., combined size fractions), which is standard practice with samples of this nature. The AMD value and the AMD ratio were calculated for each sample, using the extracted mineralogical data.

Static geochemical tests were conducted on the gold residues and one copper residue. These included ABA tests according to the modified method of Lawrence and Wang [21]. Fizz tests were additionally conducted to determine the quantity of acid required for the ABA procedure. From this, the neutralization potential (NP, expressed in kg $CaCO_3$/t) and acid generating potential (AP) were calculated (Eqs. 3.13 and 3.14):

$$NP = [(N_{HCl} \times V_{HCl}) - (N_{NaOH} \times V_{NaOH}) \times 50]/\text{mass of sample (g)} \quad (3.13)$$

Where

N is the normality (Eq/L) of HCl and NaOH, and

V is the volume (mL) HCl and NaOH

$$AP = \text{Sulfide S} \times 31.25 \quad (3.14)$$

Where

Sulfide S is determined from wet chemical analysis (LECO method), and 31.25 is a given constant to account for unit conversion

Other parameters calculated were:

Net NP (in kg $CaCO_3$/t):

$$NNP = NP - AP \quad (3.15)$$

Net acid production potential (in kg H_2SO_4/t):

$$NAPP = -NNP \times 0.98 \quad (3.16)$$

NP ratio:

$$NPR = NP/AP \quad (3.17)$$

Net acid generation (NAG) tests were additionally conducted on the samples, according to the method of Miller *et al.* [46], and the NAG was calculated as follows:

$$\text{NAG} = 49 \times V \times \text{M}/m \tag{3.18}$$

Where
NAG = net acid generation (in kg H_2SO_4/t)
V = volume of base NaOH titrated (mL)
M = molarity of base NaOH (mol/L)
m = mass of sample reacted (g)

3.3.2 Results and Discussion

Particle size distributions (PSDs) among the gold residues are, respectively, 56%, 64%, and 77% passing 75 μm for Au res 1, Au res 2, and Au res 3. The BMS 1 Tails and BMS 2 tails, representing very different mineral assemblages, are 64% and 50% passing 75 μm, respectively. The Cu res 1 tails shows a PSD around 80% passing 75 μm.

Various minerals were identified in the samples, along with calculated acid generation potentials and assigned relative reactivities (Table 3.3). AP is based on reactions of minerals with O_2 and water, releasing H_2SO_4 as the acid and therefore resulting in a positive potential. On the other hand, minerals like carbonates can consume the released acid, leading to a negative AP. As relative reactivity is assigned, it is noted that obtained acid production or consumption values are not absolute, and only comparative trends can be discussed.

Modal mineralogy and liberation data are presented for each of the six samples examined (Table 3.4). Modal mineral proportions, together with individual mineral chemical compositions, can be used to calculate a sample chemical composition. This calculated sample element composition can be compared against measured bulk assays in assessing accuracy of the modal mineral abundance. For the samples in this study, accuracy on Si, at concentrations of 25–45 mass%, was typically within 3–10% of the measured assay. For the BMS tails compositions, Mg, at concentrations of 5–15 mass%, was also within 3–10% of the measured assay. Mineral maps of particles show the associations and liberation of minerals, with liberation increasing as the particle size decreases (Figure 3.2).

The summarized results of the ABA and NAG tests, as well as the calculated AMD values and AMD ratios for each sample submitted to the geochemical tests, are also presented (Table 3.5). In this respect, it is noted that the AMD value is similar in meaning to the NAPP, as it considers the summed potential acid consuming minerals relative to summed potential acid producing minerals. Similarly, the AMD ratio may be considered equivalent to the NPR, as it considers the ratio of potential acid consuming to potential acid producing minerals. The AMD value was plotted against the NAPP, and AMD ratio against NPR, in assessing deviations between static geochemical tests and mineralogical-based predictions for each sample (Figure 3.3). The AMD values and ratios were also considered for liberation as observed, versus a calculation with liberation omitted, i.e., minerals considered all entirely liberated, in which case the liberation factor would be 1 (Table 3.6).

Table 3.3 Identified minerals in process wastes, calculated acid potential, and assigned relative reactivity.

Mineral	Formula	AP (H_2SO_4, kg/t)	Relative reactivity
Amphibole	$NaCa_2Mg_2Fe_3Si_7AlO_{22}(OH)_2$	−383	0.40
Apatite	$Ca_5(PO_4)_3(OH,F,Cl)$	0	0.004*
Calcite	$CaCO_3$	−980	1.00
Carrollite	$CuCo_2S_4$	317	1.00*
Chalcocite	Cu_2S	−616	0.07#
Chalcopyrite	$CuFeS_2$	534	0.44
Chlorite	$(Mg_3Fe_2)Al(AlSi_3O_{10})(OH)_8$	−455	0.40
Clay	$Al_2Si_2O_5(OH)_4$	0	0.02
Dolomite	$CaMg(CO_3)_2$	−1065	1.00
Fe oxide	FeO(OH)	<0	1.00*
Feldspar	$NaAlSi_3O_8$	−187	0.02
Galena	PbS	0	0.86
Muscovite	$KAl_3Si_3O_{10}(OH)_2$	−123	0.01
Pentlandite	$Ni_{4.5}Fe_{4.5}S_8$	443	1.00*
Pyrite	FeS_2	1633	1.00
Pyrophyllite	$Al_2Si_4O_{10}(OH)_2$	0	1.00*
Pyroxene	$Mg_2Si_2O_6$	−980	0.40
Pyrrhotite	Fe_7S_8	1210	8.43
Quartz	SiO_2	0	0.00
Serpentine	$Mg_3Si_2O_5(OH)_4$	−1061	0.40
Sphalerite Fe	$Zn_{0.9}Fe_{0.1}S$	145	0.96
Talc	$Mg_3Si_4O_{10}(OH)_2$	−778	0.40

*No data available; reactivity assigned based on assumed similar reactivity to pyrite, calcite, or quartz; #assigned based on observations of lower reactivity to pyrite; mineral formulae are taken from [47] and are also based on general formulae for mineral groups from [48].

Table 3.4 Modal mineral abundance (modal, mass%) and liberation (lib., % free surface) for the investigated process wastes.

Mineral	Au res 1		Au res 2		Au res 3		Cu res 1		BMS Tails 1		BMS Tails 2	
	modal	lib.	modal	lib.	modal	lib.	modal	lib.	modal	lib.	modal	lib.
Amphibole	0.1	92.8			0.3	97.2	0.4	35.2			34.5	61.1
Ankerite												
Apatite									0.3	50.3		
Calcite	0.2	99.3							0.8	56.8	1.0	67.2
Carrollite							0.3	77.8				
Chalcocite							0.6	30.5				
Chalcopyrite									0.3	73.4	0.4	72.7
Chlorite	2.5	99.4	0.3	63.4	2.6	99.7	4.4	32.2			15.7	44.0
Covellite							0.2	18.7				
Clay	0.3	n.d.					8.7	n.d.	0.7	n.d.	2.8	n.d.
Dolomite									43.8	76.1	0.7	50.2
Fe Oxides	1.1	n.d.	0.2	n.d.	0.5	n.d.	4.6		0.1	n.d.	5.6	n.d.
Feldspar	3.2	98.9	0.5	74.7	2.7	99.2	3.0		8.3	52.9	7.6	43.5
Galena									0.9	77.7		

(Continued)

Table 3.4 Modal mineral abundance (modal, mass%) and liberation (lib., % free surface) for the investigated process wastes. (*Continued*)

Mineral	Au res 1		Au res 2		Au res 3		Cu res 1		BMS Tails 1		BMS Tails 2	
	modal	**lib.**	**modal**	**lib.**	**modal**	**lib.**	**modal**	**lib.**	**modal**	**lib.**	**modal**	**lib.**
Mica	2.6	99.4	0.3	73.8	2.6	99.7	21.6	50.7	4.1	41.3	2.3	44.1
Pentlandite											0.8	67.0
Pyrite	1.9	99.9	0.5	80.7	0.2	99.8	11.2	75.9	12.8	71.8	2.1	58.4
Pyrophyllite	5.6	n.d.	2.5	n.d.	1.7	n.d.						
Pyroxene							0.1	11.2	0.6	23.1	4.3	25.4
Pyrrhotite	0.4	98.1	0.1	80.2	0.1	99.2			0.3	9.9	5.8	74.2
Quartz	82.2	n.d.	95.6	n.d.	89.4	n.d.	45.0	n.d.	25.8	n.d.	2.7	n.d.
Serpentine									0.1	51.6	6.1	28.4
Sphalerite									1.2	77.3		
Talc											7.7	34.8

n.d.: not determined. For inert minerals, liberation values were not extracted from the automated SEM data, as these values are inconsequential to the AMD value. The latter will be zero, with or without a liberation factor, as it is determined by the AP, which is zero (Table 3.3).

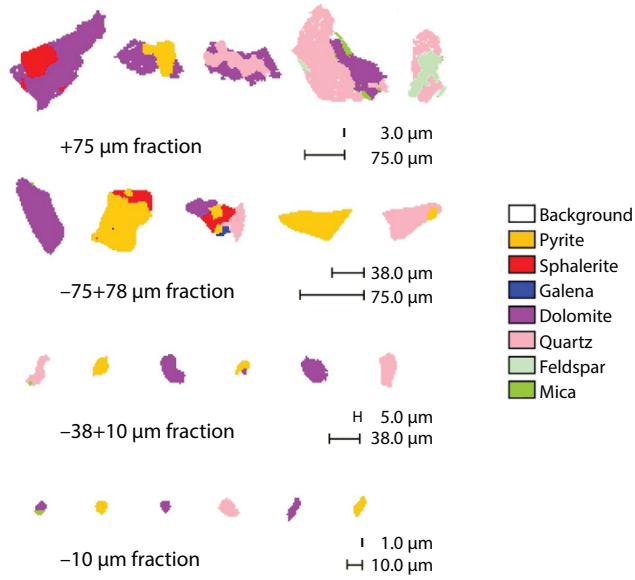

Figure 3.2 Mineral maps of selected particles from different size fractions of BMS Tails 1 analyzed by QEMSCAN, showing improved mineral liberation from coarser to finer particles.

Table 3.5 Calculated AMD parameters from static geochemical tests and mineralogical predictions on residue samples.

Sample	AMD value, kg H_2SO_4/t	AMD ratio	NNP, kg $CaCO_3$/t	NAPP, kg H_2SO_4/t	NPR	NAG pH
Au res 1	60.5	0.06	−21.3	20.83	0.15	2.23
Au res 2	15.4	0.02	3.4	−3.37	3.2	2.52
Au res 3	7.6	0.41	−2.6	2.57	0.62	3.07
Cu res 1	136.6	0.02	−145.5	142.63	0.02	2.36

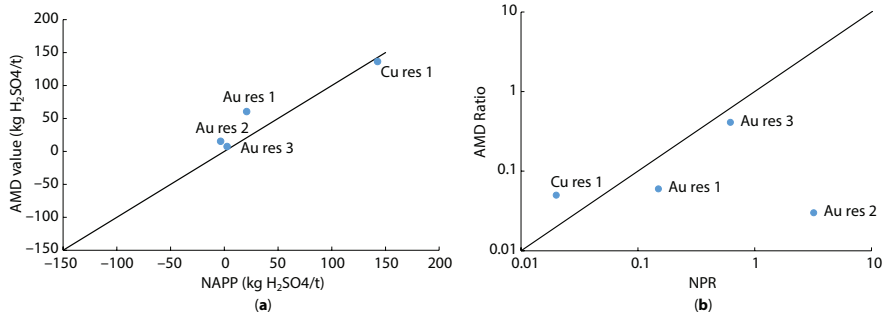

Figure 3.3 NAPP versus AMD value (a) and NPR versus AMD ratio (b) for the four samples subjected to ABA and NAG tests.

Table 3.6 Liberation (lib) effects on AMD values and ratios.

	AMD value	AMD value with lib = 1	Difference	AMD ratio	AMD ratio with lib = 1
Au res 1	60.5	61.2	0.7	0.06	0.06
Au res 2	15.4	19	3.6	0.02	0.03
Au res 3	7.6	7.7	0.1	0.41	0.41
Cu res 1	136.6	174.1	37.6	0.02	0.05
BMS Tails 1	−204.2	−233.8	29.6	2.31	1.97
BMS Tails 2	386.6	464.1	77.54	0.16	0.26

For the gold residue samples, overall, very good liberation of pyrite and pyrrhotite, as key acid producers, is observed. Silicates in these residues play virtually no role in NP, owing to the dominance of inert quartz. Differences in AMD values are due primarily to modal proportions of pyrite and pyrrhotite, as well as the pyrite:pyrrhotite ratio in influencing reactivity, given the very high reactivity assigned to pyrrhotite. Using a ranking scheme to compare the AMD values from these residues (Table 3.7), the Au res 1 residue reports to the range of values classified as extremely acid forming. Based on the ABA/NAG test classification scheme [49], this would be classified as potentially acid forming, but the relatively high pyrrhotite and pyrite content and liberation, coupled with the high reactivity of the pyrrhotite, would render the residue extremely acid forming instead.

The Au res 2 residue is acid forming, whether complete or actual liberation of pyrite and pyrrhotite is considered. Using the ABA/NAG scheme [49], this would be classified as uncertain. The Au res 3 residue is marginally lower in AMD value and is classified as potentially acid forming (Table 3.7), in agreement with ABA/NAG classification.

The Cu res 1 residue is classed as extremely acid forming (Table 3.7), owing to the high abundance of pyrite, as well as its relatively high liberation, at ≈76%. If liberation were not considered (liberation = 1, i.e., 100%), the AMD value increases substantially. The absence of carbonate, along with the presence of poorly neutralizing silicates, contributes to this high AMD value. Based on the ABA/NAG scheme, this residue is classified as potentially acid forming, but from the ABA/NAG scheme [49], it is high risk acid generating.

For the compositions of BMS tailings, composition BMS Tails 1 is potentially alkaline generating, owing to the dominance of reactive dolomite, compared with pyrite as the dominant sulfide. As the same reactivity is assigned, and both display similar liberation, the modal proportions become the key factor in determining the AMD value. Where complete liberation is assumed, the AMD value would decrease substantially; this appears to be more prevalent where liberation is typically <70% (Tables 3.4 and 3.6). Composition BMS Tails 2 is extremely acid producing, with a substantial increase in AMD value with complete liberation assumed, again because of liberation typically <70% for most minerals. Relatively high content of highly reactive pyrrhotite, along with good liberation, accounts for the classification. Reactive silicates, despite their abundance, cannot mitigate the effects of the reactive pyrrhotite in this instance.

Table 3.7 Classification based on the AMD value (Eq. 3.11).

AMD value	Classification
<–100	Potentially alkaline generating
–100 to –50	Acid neutralizing
–50 to –10	Inert
–10 to +10	Potentially acid forming
+10 to +50	Acid forming
>+50	Extremely acid forming

Table 3.8 Classification based on the AMD ratio (Eq. 3.12).

AMD ratio	Classification
<0.1	Extremely high risk of AMD
0.1 to 0.5	High risk of AMD
0.5 to 1.0	Risk of AMD
1.0 to 5	Low risk of AMD
5 to 10	Very low risk of AMD
>10	No risk of AMD

In terms of the AMD ratio, the smaller the effect of the acid consumers on the AMD value, the smaller the AMD ratio. Given the absence of carbonate in three of the residues, along with very small contribution from neutralizing silicates, these report to the extremely high risk of AMD formation class (Table 3.8). Note that this is not an indication of how much AMD could form but the risk of it forming. One gold residue and one of the BMS tailings composition report to the high risk of AMD formation class, and the tailings composition high in dolomite reports to the low risk of AMD formation class. The AMD ratios do not change dramatically with a full liberation assumed, compared with measured liberation.

The examples illustrate a complex interplay of mineral type (acid producer, neutralizer, inert), mineral proportion, reactivity (oxidation rate versus acid consumption reactivity), and liberation in contributing to the amount of acid that may be produced by a waste sample, as well as the risk of that acid being produced. The addition of reactivity and liberation to mineral proportions brings a kinetic aspect to the determination of AMD potential.

Based on the general particle size representing process wastes in this study, it is evident that mineral liberation plays a vital role in quantifying exposed surface available for mineral reactivity. As particle size increases relative to the grain size of the minerals in the particles of a given ore, liberation will approach zero, because less surface is typically exposed (Figures 3.1 and 3.2). In such a case (e.g., particle size at the mm scale, containing mineral

grains at the micron scale), liberation decreases, and thus, the potential and risk to form AMD is decreased. The difference in AMD value using measured liberation (i.e., liberation <1) as opposed to full liberation (i.e., liberation = 1) is particularly pronounced in the BMS process wastes in this study (Table 3.6). This will be a function of the mineral grain size distribution at the PSD studied. Mineral grain size distribution is a function of the original texture of the ore. Larger grains in the original ore liberate at coarser particle sizes than smaller grains. This therefore gives rise to potentially different mineral liberation properties for a given PSD of two different ores or waste compositions containing the same mineral. Reaction kinetics will be consequently affected.

As part of a geometallurgical approach, feed material to a process will have a given PSD and particle tracking models have been developed to help simulate the behavior of such particles in the process [50]. Which particles will report to the tails is a key consideration in optimizing grade and recovery to the concentrate and forms a cornerstone of many process mineralogical investigations. Using this approach from the angle pursued in this study, the same said particles reporting to the final tails after optimization for recovery of value should be assessed for the potential to produce acid over time. Indeed, current efforts are aimed at desulfurization processes, in which bulk sulfide flotation of tailings streams is considered to "clean" the tailings of residual sulfides and the resultant material can be used as cover over tailings storage facilities [51, 52]. This is costly and should be a process design consideration upfront rather than a mitigation option after processing.

Analysis of a judiciously selected set of samples can yield information pertinent to not only process efficiency (grade and recovery optimization versus market conditions and mining plan progression) but also tailings production (AMD potential, considering environmental conditions for the tailings storage facility and temporal changes). Indeed, design considerations would aim at integrated strategies for both process efficiency optimization and AMD mitigation. In this respect, detailed mineralogical information would not come at extra cost, as the ore deposit definition will be serving multiple purposes and will provide more value to the operations from a prediction perspective.

3.4 Conclusions and Further Work

To complement traditional static geochemical tests, an approach using mineral proportions, mineral acid production or consumption potential, mineral reactivity, and mineral liberation was applied for the prediction of AMD potential of gold and copper process residues, as well as BMS tailings compositions, representing process wastes. The mineral reactivity, together with relative abundance, plays a major role in determining AMD values of samples. Liberation appears to be an important factor when minerals occur with exposure less than 70%. Abundance of higher reactivity silicates like chlorite, amphibole, and talc may be more influential over time but are unlikely to mitigate more immediate sulfide reaction.

Mineral proportions and liberation data were obtained using automated scanning electron microscopy techniques, with a database developed for mineral acid production or consumption potential and mineral reactivity. It should be noted that certain assumptions are made where published information on the latter two parameters is sparse. Nevertheless, comparative analysis is possible and provides an indication of AMD potential. As empirical

data are obtained from test work and complemented by mineral chemical compositional information, the database can be strengthened through addition of observed values for use with quantitative mineralogy.

The approach has application in the prediction of AMD potential of process wastes which typically show particle sizes in the micron range. At these particle sizes, liberation effects of acid producing sulfides are more pronounced than at the centimeter or meter scales of waste rock and therefore will influence the acid production potential of the waste.

Although mineralogical observations have also aided in the understanding of changes during kinetic or long-term testing [17, 18], these observations presently do not predict how much acid will be formed, and when, if at all. Building on the concepts around liberation and mineral reactivity presented here, work is underway on iterative modeling and simulation of changing particle properties over time. As an example, a strong acid producer, where liberated, should produce acid faster than the same strong acid producer locked entirely within a poorly reactive silicate, based on the surface area available for oxidation. This concept would be suited to prediction of AMD production over time for process wastes, and finer particles of waste rocks (e.g., –3 mm) and would be a desirable alternative to time-consuming and costly kinetic tests that are presently performed. Consideration of the sulfide suite of minerals, together with liberation and association information, should yield clues on the extent to which galvanic interaction may be expected, and their contribution to possible passivation effects. Together with the modeling of environmental effects like temperature and fluid flow dynamics the outcomes present an attractive alternative to costly and time-consuming kinetic tests to predict how much AMD will form, and when.

Acid mine drainage prediction studies should form part of an integrated strategy that optimizes process efficiency while mitigating environmental problems so that sustainable operations may be pursued in line with, and as part of, a geometallurgical program. The consideration of mineralogy, mineral modal abundance, mineral reactivity, and mineral liberation, as added in this work, should improve these predictive studies.

References

1. Sutton, P.A., Perspective on environmental sustainability? A paper for the Victorian Commissioner for Environmental Sustainability, 2004. http://www.green-innovations.asn.au/A-Perspective-on-Environmental-Sustainability.pdf.
2. Younger, P.L., Banwart, S.A., Hedin, R.S., *Mine Water – Hydrology, Pollution, Remediation*, p. 464, Kluwer, Dordrecht, 2002.
3. Wolkersdorfer, C., *Water Management at Abandoned Flooded Underground Mines – Fundamentals, Tracer Tests, Modelling, Water Treatment*, p. 465, Springer, Heidelberg, 2008.
4. Jamieson, H.E., Walker, S.R., Parsons, M.B., Mineralogical characterization of mine waste. *Appl. Geochem.*, 57, 85–105, 2015.
5. Dold, B., Acid rock drainage prediction: A critical review. *J. Geochem. Expl.*, 172, 120–132, 2017.
6. McCarthy, T.S., The impact of acid mine drainage in South Africa. *S. Afr. J. Sci.*, 107, 5/6, 7, 2011. Art. #712, https://doi.org/10.4102/sajs.v107i5/6.712, 2011.
7. van Rooyen, M., Acid Mine Drainage Water Treatment using the SAVMIN Process, in: *SAIMM Hydrometallurgy 2016*, pp. 52–60, South African Institute of Mining and Metallurgy, Cape Town, South Africa, 2016.

8. Masindi, V., Madzivire, G., Tekere, M., Reclamation of water and the synthesis of gypsum and limestone from acid mine drainage treatment process using a combination of pre-treated magnesite nanosheets, lime and CO_2 bubbling. *Water Resour. Ind.*, 20, 1–14, 2018.
9. Parbhakar-Fox, A.K., Edraki, M., Walters, S., Bradshaw, D., Development of a textural index for the prediction of acid rock drainage. *Miner. Eng.*, 24, 1277–1287, 2011.
10. Parbhakar-Fox, A., Lottermoser, B.G., Bradshaw, D., Evaluating waste rock mineralogy and microtexture during kinetic testing for improved acid rock drainage prediction. *Miner. Eng*, 52, 111–124, 2013.
11. Parbhakar-Fox, A., Lottermoser, B., Hartner, R., Berry, R.F., Noble, T.L., Prediction of Acid Rock Drainage from Automated Mineralogy, in: *Environmental Indicators in Metal Mining*, B. Lottermoser (Ed.), pp. 139–156, Springer, Cham, 2017, https://doi.org/10.1007/978-3-319-42731-7_8.
12. Parbhakar-Fox, A. and Lottermoser, B.G., A critical review of acid rock drainage prediction methods and practices. *Miner. Eng.*, 82, 107–124, 2015.
13. Becker, M., Dyantyi, N., Broadhurst, J.L., Harrison, S.T.L., Franzidis, J.P., A mineralogical approach to evaluating laboratory scale acid rock drainage characterization tests. *Miner. Eng.*, 80, 33–36, 2015.
14. Jambor, J.L., Dutrizac, J.E., Groat, L.A., Raudsepp, M., Static tests of neutralization potentials of silicate and aluminosilicate minerals. *Environ. Geol.*, 43, 1–17, 2002.
15. Paktunc, A.D., Mineralogical constraints on the determination of neutralization potential and prediction of acid mine drainage. *Environ. Geol.*, 39, 103–112, 1999.
16. Abrosimova, N., Gaskova, O., Loshkareva, A., Edelev, A., Bortnikova, S., Assessment of the acid mine drainage potential of waste rocks at the Ak-Sug porphyry Cu–Mo deposit. *J. Geochem. Expl.*, 157, 1–14, 2015.
17. Brough, C., Strongman, J., Bowell, R., Warrender, R., Prestia, A., Barnes, A., Fletcher, J., Automated environmental mineralogy; the use of liberation analysis in humidity cell testwork. *Miner. Eng.*, 107, 112–122, 2017.
18. Brough, C., Parbhakar-Fox, A., Fletcher, J., Barnes, A., Griffiths, R., Strongman, J., Bowell, R., Garner, C., Becker, M., Automated Environmental Analysis: Multiple size fraction analysis of kinetic tests and implications for geochemical interpretations, in: *Proceedings: Process Mineralogy 18 conference*, MEI, Cape Town, 2018.
19. Sobek, A.A., Schuller, W.A., Freeman, J.R., Smith, R.M., *Field and Laboratory Methods Applicable to Overburdens and Minesoils*, p. 203, U.S. Environmental Protection Agency, EPA, Washington, D.C., 600-2-78–054, 1978.
20. Lawrence, R.W., Prediction of the behaviour of mining and processing wastes in the environment, in: *Proceedings, Western Regional Symposium on Mining and Mineral Processing Wastes.* F. Doyle (Ed.), pp. 115–121, Society for Mining, Metallurgy, and Exploration, Littleton, CO, 1990.
21. Lawrence, R.W. and Wang, Y., Determination of Neutralization Potential in the Prediction of Acid Rock Drainage, in: *Proceedings of the 4th International Conference on Acid Rock Drainage*, pp. 449–464, Vancouver, BC.1997.
22. Lapakko, K., Evaluation of neutralization potential determinations for metal mine waste and a proposed alternative, in: *Proc. International Land Reclamation and Mine Drainage Conference*, pp. 129–137, 1994, https://doi.org/10.21000/JASMR94010129.
23. Maest, A.S., Kuipers, J.R., Travers, C.L., Atkins, D.A., *Predicting Water Quality at Hardrock Mines: Methods and Models, Uncertainties, and State-of-the-Art*, Kuipers & Associates and Buka Environmental, Washington, D.C., 2005.
24. Perkins, E.H., Nesbitt, H.W., Gunter, W.D., St-Arnaud, L.C., Mycroft, J.R., *Critical review of geochemical processes and geochemical models adaptable for prediction of acid drainage from waste rock*, p. 283, MEND report, Ontario, 1995.

25. Parbhakar-Fox, A., *Establishing the benefit of an integrated geochemistry-mineralogy-texture approach for acid rock drainage prediction*, PhD thesis, University of Tasmania, 2012.
26. Nordstrom, D.K., Blowes, D.W., Ptacek, C.J., Hydrogeochemistry and microbiology of mine drainage: An update. *Appl. Geochem.*, 57, 3–16, 2015.
27. Chopard, A., Benzaazoua, M., Plante, B., Bauzahzan, H., Marion, P., Kinetic Tests to Evaluate the Relative Oxidation Rates of Various Sulfides and Sulfosalts, in: *Proceedings, 10th International Conference on Acid Rock Drainage and IMWA annual conference*, 2015.
28. Stanton, M.R., Taylor, C.D., Gemery-Hill, P.A., Shanks, W.C. III, Laboratory studies of sphalerite decomposition: Applications to the weathering of mine wastes and potential effects on water quality, in: *The 7th International Conference on Acid Rock Drainage (ICARD)*, R.I. Barnhisel (Ed.), The American Society of Mining and Reclamation (ASMR), Lexington, KY, 2006.
29. Plumlee, G.S., The Environmental Geology of Mineral Deposits, in: *The Environmental Geochemistry of Mineral Deposits, Part A: Processes, Techniques and Health Issues*, vol. 6A, G.S. Plumlee and M.J. Logsdon (Eds.), pp. 71–116, Society of Economic Geologists, Littleton, Colorado, Reviews in Economic Geology, 1999.
30. The International Network for Acid Prevention (INAP), Global Acid Rock Drainage Guide (GARD Guide), 2009. http://www.gardguide.com.
31. Dold, B., Evolution of Acid Mine Drainage Formation in Sulphidic Mine Tailings. *Minerals*, 4, 621–641, 2014.
32. Edraki, M., Baumgartl, T., Manlapig, E., Bradshaw, D., Designing mine tailings for better environmental, social and economic outcomes: A review of alternative approaches. *J. Clean. Prod.*, 84, 411–420, 2014.
33. Khorasanipour, M., Environmental mineralogy of Cu-porphyry mine tailings, a case study of semi-arid climate conditions, Sarcheshmeh mine, SE Iran. *J. Geochem. Explor.*, 153, 40–52, 2015.
34. Moncur, M.C., Ptacek, C.J., Lindsay, M.B.J., Blowes, D.W., Jambor, J.L., Long-term mineralogical and geochemical evolution of sulfide mine tailings under a shallow water cover. *Appl. Geochem.*, 57, 178–193, 2015.
35. Jambor, J.L., Ptacek, C.J., Blowes, D.W., Moncur, M.C., Acid drainage from the oxidation of iron sulfides and sphalerite in mine wastes, in: *Proceedings from: Lead & Zinc '05*, vol. 1, T. Fujisawa (Ed.), The Mining and Materials Processing Institute of Japan, Tokyo, 2005.
36. Aspandiar, M.F. and Eggleton, R.A., Weathering of Chlorite: I. Reactions and Products in Microsystems Controlled by the Primary Mineral. *Clay Clay Miner.*, 50, 685–698, 2002.
37. Dos Santos, E.G., de Mendonça Silva, J.C., Duarte, H.A., Pyrite Oxidation Mechanism by Oxygen in Aqueous Medium. *J. Phys. Chem.*, 120, 2760–2768, 2016.
38. Gottlieb, P., The revolutionary impact of automated mineralogy on mining and mineral processing, in: *24th International Mineral Processing Congress*, pp. 165–174, Science Press, Beijing, 2008.
39. Fandrich, R., Gu, Y., Burrows, D., Moeller, K., Modern SEM-based mineral liberation analysis. *Int. J. Miner. Process.*, 84, 310–320, 2007.
40. Sverdrup, H.U., *The kinetics of base cation release due to chemical weathering*, Lund University Press, Lund, 246 pp, 1990.
41. Kwong, Y.T.J., *Prediction and prevention of acid rock drainage. MEND project*, p. 47, Canadian Centre for Mineral and Energy, Ottawa, 1993.
42. Noble, T.L. and Lottermoser, B.G., Modified Abrasion pH and NAG pH Testing of Minerals. *Environ. Indic. Met. Mining*, 19 October 2016, 211–220, 2016.
43. Bouzahzah, H., Benzaazoua, M., Bussiere, B., Plante, B., Prediction of Acid Mine Drainage: Importance of Mineralogy and the Test Protocols for Static and Kinetic Tests. *Mine Water Environ.*, 33, 54–65, 2014.

44. Chopard, A., Benzaazoua, M., Bouzahzah, H., Plante, B., Marion, P., A contribution to improve the calculation of the acid generating potential of mining wastes. *Chemosphere*, 175, 97–107, 2017.
45. Goodall, W.R., Scales, P.J., Butcher, A.R., The use of QEMSCAN and diagnostic leaching in the characterisation of visible gold in complex ores. *Miner. Eng.*, 18, 877–886, 2005.
46. Miller, S., Robertson, A., Donahue, T., Advances in Acid Drainage Prediction Using the Net Acid Generation (NAG) Test, in: *Proceedings of the 4th International Conference on Acid Rock Drainage*, pp. 533–549, 1997.
47. Mineralogy Database: http://www.webmineral.com
48. Deer, W.A., Howie, R.A., Zussman, J., *An Introduction to the Rock-Forming Minerals*, 2nd edition, p. 696, Longman Scientific and Technical, New York, 1992.
49. De Wet, L., Acid base accounting of mining ore and waste. *Test Meas. Conf.* 2012. September, http://nla.org.za/webfiles/conferences/2012/Presentations
50. Lamberg, P. and Vianna, S.M.S., A technique for tracking multiphase mineral particles in flotation circuits, in: *VII meeting of the southern hemisphere on mineral technology*, pp. 195–203, Ouro Preto, 2007.
51. Skandrani, A., Demers, I., Kongolo, M., Desulfurization of aged gold-bearing mine tailings. *Miner. Eng.*, 138, 195–203, 2019.
52. Benzaazoua, M., Bouzahzah, H., Taha, Y., Kormos, L., Kabombo, D., Lessard, F., Bussi, B., Demers, I., Kongolo, M., Integrated environmental management of pyrrhotite tailings at Raglan Mine: Part 1 challenges of desulphurization process and reactivity prediction. *J. Clean. Prod.*, 162, 86–95, 2017.